

Published in final edited form as:

IEEE Trans Biomed Eng. 2008 November ; 55(11): 2557–2564. doi:10.1109/TBME.2008.919885.

Estimation of time-varying connectivity patterns through the use of an adaptive directed transfer function

C. Wilke [Student Member, IEEE], L. Ding [Member, IEEE], and B. He [Fellow, IEEE]*

Department of Biomedical Engineering, University of Minnesota

Abstract

Frequency-derived identification of the propagation of information between brain regions has quickly become a popular area in the neurosciences. Of the various techniques used to study the propagation of activation within the central nervous system, the directed transfer function (DTF) has been well used to explore the functional connectivity during a variety of brain states and pathological conditions. However, the DTF method assumes the stationarity of the neural electrical signals and the time invariance of the connectivity among different channels over the investigated time window. Such assumptions may not be valid in the abnormal brain signals such as seizures and interictal spikes in epilepsy patients. In the present study, we have developed an adaptive DTF method (ADTF) through the use of a multivariate adaptive autoregressive model to study the time-variant propagation of seizures and interictal spikes in simulated electroencephalogram (ECoG) networks. The time-variant connectivity reconstruction is achieved by the Kalman filter algorithm which can incorporate time-varying state equations. We study the performance of the proposed method through simulations with various propagation models using either sample seizures or interictal spikes as the source waveform. The present results suggest that the new ADTF method correctly captures the temporal dynamics of the propagation models while the DTF method cannot, and even returns erroneous results in some cases. The present ADTF method was tested in real epileptiform electroencephalogram data from an epilepsy patient and the ADTF results are consistent with the clinical assessments performed by neurologists.

Keywords

DTF; adaptive DTF; connectivity; epilepsy

1. Introduction

Frequency-based analysis techniques of electrical signals recorded from the brain are popular among the neuroscience community due to the inherent spectral encoding of brain activities. Such techniques are often utilized in the identification and characterization of the propagation of information between brain regions during different brain states or in a variety of pathological conditions [1]. Before the advent of most functional imaging modalities, knowledge of communication between areas of the brain was limited to knowledge of the anatomical connections between them. Nowadays, neuroscientists utilize advanced imaging and signal processing techniques to better understand the intricacies of the functional connectivity of the brain [2–4].

*Correspondence: Bin He, Ph.D., University of Minnesota, 7-105 NHH, 312 Church Street, SE, Minneapolis, MN 55455; E-mail: binhe@umn.edu.

Much of the work performed in the study of interactions between brain regions has used bivariate measures, such as the analysis of coherence between recordings from different brain areas [5,6]. The limitation, however, of coherence analysis is that there exists no information regarding the direction of the functional coupling. Furthermore, bivariate measures could be potentially misleading when applied to multivariate systems [7]. To overcome this shortcoming, Kaminski and Blinowska proposed the directed transfer function (DTF) as a method to extract the directional information flow between brain structures [8]. Derived from the coefficients of a multivariate autoregressive (MVAR) model fit to the data, the DTF can be used to handle multi-channel signals and can be thought of as a type of multivariate Granger causality [9].

In previous studies, investigators have shown that the DTF can be used to localized epileptogenic foci in patients with partial epilepsy [10–12]. In some of these studies, the DTF method was applied to intracranial recordings of seizures in patients undergoing surgical evaluation for the treatment of intractable epilepsy. The investigators found that electrodes identified by the DTF as primary sources were highly correlated with the areas of cortex identified by physicians as the seizure onset zones. However, a drawback of the DTF method, as well as other connectivity estimators which use MVAR coefficients, requires the assumption that the signals are stationary and the connectivity pattern among them is unchanged over the analyzed time period [8]. In some early studies, the stationarity of the data was judged by visual analysis [10]. Given the dynamic nature of neural activity, such an assumption might not always be valid, especially for events which are temporally short, as in the case of interictal spikes. Thus, the DTF method may not catch time-variant connectivity, and violation of such an assumption may lead to a possible erroneous reconstruction of connectivity patterns and create a misinterpretation of the propagation of interictal and seizure activity. In such a situation, a method which could identify the temporal dynamics of the connectivity pattern is greatly needed and could serve to provide a useful analytical tool.

In the present study, we have developed a new adaptive DTF (ADTF) method to reconstruct the time-variant connectivity pattern by analyzing time-varying coefficients obtained from a multivariate adaptive autoregressive (MVAAR) model. We first examine the performance of the ADTF method in extracting the time-variant propagation of activity in various simulated models with both seizure and interictal spike data as inputs. We also calculate the DTF-derived connectivity patterns and compare them to the ADTF results. Finally, we apply the ADTF method to electroencephalogram (ECoG) recordings of interictal spikes in a patient undergoing surgical evaluation for intractable epilepsy and compare the results with those from the clinical assessment.

II. Methods

A. Multivariate Adaptive Autoregressive (MVAAR) Modeling

For each time series, a MVAAR model was constructed and used to describe the dataset as follows:

$$X(t) = \sum_{i=1}^p \Lambda(i,t)X(t-i) + E(t) \quad (1)$$

Where $X(t)$ is the data vector over time, $\Lambda(i,t)$ are the matrices of time-varying model coefficients, $E(t)$ is multivariate independent white noise and p is the model order. We established the time-varying coefficient matrices by the Kalman filter algorithm [13] which describes the behavior of the multivariate signals by the observations equation, i.e. Eq. (1), and the following state equation:

$$\Lambda(i,t) = \Lambda(i,t-1) + V(i,t-1) \quad (2)$$

The observation and state equations of this algorithm can be solved by the recursive least squares (RLS) algorithm with forgetting factor [14]. The optimum order for the model was chosen by the Schwarz Bayesian Criterion (SBC) [15] which has previously been shown to possess a high degree of accuracy [16].

B. Adaptive Directed Transfer Function (ADTF)

The DTF function, $H(f)$, can be obtained from the MVAR model and is described by transforming Eq. (1), where Λ is a function of t , into the frequency domain. The DTF is computed by:

$$\Lambda(f)X(f)=E(f) \quad \text{where } \Lambda(f)=\sum_{k=0}^p \Lambda_k e^{-j2\pi f \Delta t k} \quad (3)$$

$$X(f)=\Lambda^{-1}(f)E(f)=H(f)E(f) \quad (4)$$

where $\Lambda_{k=0} = I$. Since we are able to characterize the time-varying model coefficients, $\Lambda(i,t)$, the function $H(f,t)$ can thus be obtained from the time-varying transfer matrix. Its elements, H_{ij} , represent the connection between the j^{th} and i^{th} elements of the system for each time point t . Similarly to the DTF function in Eq. (4) [8], the normalized ADTF is defined by the elements of the transfer matrix in the spectral domain, which describes the directional causal interaction from the j^{th} to the i^{th} element as:

$$\gamma_{ij}^2(f,t)=\frac{|H_{ij}(f,t)|^2}{\sum_{m=1}^n |H_{im}(f,t)|^2} \quad (5)$$

In order to evaluate the total information flow from a single node, we define the so-called integrated ADTF by summing the ADTF values over the frequency bands of interest. These bands are selected as corresponding to the seizure or interictal spike frequencies. The integrated ADTF over the frequency bands is normalized to be between (0,1).

$$\Theta_{ij}^2(t)=\frac{\sum_{k=f_1}^{f_2} \gamma_{ij}^2(k,t)}{f_2 - f_1} \quad (6)$$

The total information outflow from each node is further given by summing across subscript i for each j^{th} node and is normalized by dividing by the number of outflow nodes:

$$\Phi_j^2(t)=\frac{\sum_{k=1}^n \Theta_{kj}^2(t)}{n-1} \quad \text{for } k \neq j \quad (7)$$

The total information outflow corresponds to the degree in which activity propagates from a particular node to the rest of the network. A total outflow value of one indicates a high degree of source activity while an outflow value around zero indicates that the particular node has little to no source activity for a given time series.

C. Surrogate Data Testing

The DTF and ADTF functions have a highly nonlinear relationship to the time series from which they are derived. As such, the distribution of their estimators under the null hypothesis of no connectivity is not well established and parametric statistical analysis cannot be used. To overcome this problem, a nonparametric statistical test using surrogate data [17,18] was utilized in the present study. In this method, the phases of the Fourier coefficients were

randomly and independently shuffled to produce a new surrogate time series. This procedure of shuffling the phases of the Fourier coefficients preserves the spectral structure of the time series which is a critical aspect since the DTF and ADTF are measures of frequency-specific causal interactions. The shuffling procedure was repeated 1000 times for each model-derived time series in order to create an empirical distribution of DTF or ADTF values under the null hypothesis of no causal interactions. Using this distribution, the statistical significance of the DTF and ADTF values from the original time series was evaluated [12].

D. Model Construction for Simulation

Three time-varying causal models were created to test the performance of the ADTF method and their results are compared with those obtained from the conventional DTF approach. Each model simulated cortical potential signals recorded by ECoG electrodes, where a sample recording of a seizure or interictal spike was input into a channel and then propagated to the other channels based upon the simulated connectivity pattern.

The first model consisted of two nodes in which a sample seizure recording was input to the first node and was then propagated to the second node based upon one of three propagation patterns. The general form of the first model was as follows:

$$\begin{aligned}x_1(t) &= \phi(t) + \varepsilon(t) \\x_2(t) &= \alpha \cdot x_1(t-1) + \beta \cdot x_2(t-1) + \gamma \cdot x_2(t-3) + \varepsilon(t)\end{aligned}\quad (8)$$

where $\phi(t)$ was the sample seizure waveform, $\varepsilon(t)$ was independently distributed Gaussian white noise and α , β , and γ were the weighting coefficients with values chosen between $(-1,1)$. The sample seizure waveform was obtained from an intracranial recording in an epilepsy patient, and consisted of a three second time series taken from a representative channel and sampled at 400 Hz.

For the first connectivity pattern, there was initially no propagation between node 1 and node 2 (i.e. $\alpha = 0$). That is, for the initial segment of the time series, node 1 consisted of the seizure signal and noise while node 2 contained only noise. Midway through the sample recording ($t = 1.5$ s), the connectivity pattern was changed such that there was a propagation from node 1 to node 2 (i.e. $\alpha > 0$). In the second connectivity pattern, the interaction between node 1 and node 2 was modeled as a Gaussian distribution where the weighting factor, α , took the form of a normal distribution centered at the 1.5 s time mark and a standard deviation of 0.5 s. This pattern was used to simulate the transient flow of information during a short time segment. Finally, for the third connectivity pattern, the model was constructed as an oscillatory system in which the seizure signal alternated as propagating from node 1 to node 2 to subsequently propagating from node 2 to node 1 at a frequency of 1 Hz. Bivariate time series were constructed for the three connectivity patterns with a signal to noise ratio (SNR) of 20, 15, 10 and 5 dB for each pattern.

The second model which was examined consisted of a 3×3 grid in which a sample interictal spike was input into the center node (node 5) and then propagated in an outward manner (Fig. 1). This model was designed to simulate the spread of an interictal spike across ECoG grid electrodes under two different connectivity patterns. In the first connectivity pattern, the interactions among the nodes were assumed to be static over the length of the time series. In the second connectivity pattern, interaction among the nodes was assumed to be transient. We hypothesized that the information flow only occurred during the interictal spike and was proportional to the strength of the signal. For this purpose we used a Gaussian distribution with a standard deviation matched to approximate the duration of the interictal spike in order to create the connectivity weighting coefficients. This pattern was similar to that of the second connectivity pattern of the first model.

The third model consisted of a 2×2 grid designed to simulate the movement of a primary seizure focus to a secondary generator. The sample seizure recording used in the first model was input into the third node and propagated to the remaining nodes (Fig. 2(a)). Midway through the recording, the location of this seizure “focus” was switched and the second node became the primary source (Fig. 2(b)).

Since the model orders were predefined in the simulations, the SBC was used as a validation check of the chosen order of the MVAR/MVAAR models. A model order of 3 was used in the construction of the first model, while the second and third models both used second order MVAR/MVAAR models. Significance testing using the surrogate data method was performed for the calculated DTF and ADTF values.

E. Experimental Data Acquisition and Analysis Protocol

In addition to the models previously described, the ADTF was applied to several interictal spikes obtained from an epileptic patient. Recordings were obtained from an 8×8 subdural grid covering portions of the frontal, parietal and temporal lobes. The ECoG data was sampled at 400 Hz and band-pass filtered from 1–100 Hz. Channels were visually inspected and those which contained artifact were discarded from the analysis. The optimal model order was selected by the SBC and ranged from 3 to 6. An example of the SBC result for a representative spike is shown in Fig. 3(a). The frequency band of interest was chosen by visual inspection of a time-frequency construction of the time series and was typically around 6–9 Hz for ictal data and consisted of a slightly larger band for spike data (Fig. 3(b)). Total information outflow, as described in Eq. (7), was calculated for the ECoG grid electrodes. Nodes exhibiting the most outflow were regarded as the primary source(s) and compared to the epileptogenic foci determined clinically.

III. Results

A. Simulated Models

The DTF and ADTF values were calculated from the three models described previously. The significant DTF/ADTF values as determined by surrogate data testing were integrated in order to obtain the total information outflow, Φ , for each node. The outflow from each of the two nodes in the first model for the first connectivity pattern of the first model is shown in Fig. 4. Here it can be seen that both the DTF and ADTF methods identify node 1 as the primary source of the seizure activity since it has the most significant information outflow over the entire time window. Note that since the DTF is time-invariant, the total information outflow calculated using this method is constant over the length of the time series. It can further be seen from Fig. 4 that while both the DTF and ADTF methods identify the first node as the primary source, only the time-variant ADTF captures the dynamics of the system. The results for both the DTF and ADTF for the time series with SNRs of 15, 10 and 5 dB (waveforms not shown) were similar to those shown in Fig. 4.

Similar to the first connectivity pattern, the outflow calculated using both the DTF and ADTF methods (at 20 dB) for the second connectivity pattern identified the first node as the primary source of the seizure activity (Fig. 5). The ADTF was correctly able to identify the dynamic nature of the propagation, which is a Gaussian shape centered at 1.5 s. The results obtained from the time series with SNRs of 15, 10 and 5 dB (waveforms not shown) are analogous to those shown in Fig. 5.

The results obtained from the third connectivity pattern with a SNR of 20 dB are shown in Fig. 6. The DTF method shows significant outflow from both nodes 1 and 2. The ADTF method also depicts information outflow from node 1 and node 2 and, furthermore, captures the

oscillating dynamics of the connectivity pattern as the outflow alternates between the two nodes. While similar results were obtained with a SNR of 15 dB, the DTF returned significant outflow from only the first node with SNRs of 10 and 5 dB. The ADTF results were similar under all four SNR levels.

The total outflow was also calculated for the two connectivity patterns used in the second model (Fig. 7–Fig. 8). In the first pattern (Fig. 7), since the connectivity coefficients are constant, the total outflow from both the DTF and ADTF methods identified node 5 as the primary source of propagation of the interictal spike activity. This relationship was also true for the time series calculated with SNRs of 15, 10 and 5 dB. In the second pattern (Fig. 8), the connectivity coefficients were weighted according to a Gaussian distribution similar to that performed in the second causal pattern in the first model. The peak of the connectivity strength was set at the time point of the peak of the interictal spike. It can be seen that the majority of the significant information outflow calculated using the ADTF method occurs from channel 5 which is in agreement with the model (Fig. 8(a)). The significant outflow calculated using the DTF, however, identifies node 2 as having the greatest amount of outflow. For the other SNR values, node 5 always had the highest amount of outflow when calculated using the ADTF method. Use of the time-invariant DTF, however, identified several other nodes in addition to the fifth node which displayed the maximum significant outflow at the three other SNR levels (Table 1). These errors in outflow as calculated by the DTF are likely due to the fact that the conventional DTF method is time-invariant and cannot incorporate the dynamic connectivity information of the model. Thus, from the results in Fig. 7 as well as Table 1, it can be seen that when the connectivity pattern is static, both the ADTF and DTF methods function equivalently (ie. they both correctly identify the source node). However, when the connectivity pattern is time-variant, the ADTF method correctly identifies the source node as having the highest amount of outflow whereas the DTF method identifies “false sources” with significant outflow greater than the true source of propagation (see Fig. 8 and Table 1).

The total outflow from each node in the third model using both the DTF and ADTF methods is shown in Fig. 9. In the third model, the “foci” from which the seizure signal propagates, switches from node 3 to node 2 midway through the time series. It can be observed that the total information outflow calculated using the ADTF method shows information propagating from node 3 during the first half of the time series which then switches to node 2 during the later portion of the time series. For the total information outflow calculated using the DTF method, both nodes 2 and 3 exhibit significant outflow. The results for both the ADTF and DTF methods were similar for all four investigated SNR levels.

B. ECoG Data of Interictal Spikes from an Epilepsy Patient

The ADTF method was also applied to four interictal spikes recorded from a patient undergoing long-term monitoring for surgical evaluation of intractable epilepsy. The results for one spike are shown in Fig. 10. Here, the brain regions identified by the epileptologist during the presurgical evaluation as belonging to the epileptogenic zone are marked in red (Fig. 10(a)). In this patient, there were two clinically-identified zones: one in the superior temporal/inferior parietal region and the other in the frontal lobe. Of the four spikes investigated, however, the waveforms were not observed in the area of the frontal focus. Representative waveforms for the two regions are shown in Fig. 10(a). In this figure, the electrodes identified by the ADTF method as having the greatest amount of information outflow during the interictal spike are highlighted. The temporal time courses of the ADTF values from these electrodes are shown in Fig. 10(b). As can be seen from this figure, the information outflow from those electrodes correlates well with the time course of the interictal spike. The locations of the ADTF-identified sources for the remaining three interictal spikes are shown in Fig. 11. All of the identified sources lie within or adjacent to the temporal focus and have ADTF time courses similar to

that shown in Fig. 10(b). Conventional DTF analysis was also performed on the interictal spike data (data not shown). However, the nodes identified through this analysis as the sources of information outflow were not consistent in location among the spikes nor were they co-localized with the seizure onset zone determined by the clinicians.

IV. Discussion

In this paper, we have examined an adaptive directed transfer function method based upon the MVAAR model in the context of seizure and interictal spike propagation. We have tested the performance of the algorithm in various conditions simulating seizure and interictal spike propagation with predefined patterns and have compared its performance to the conventional (time-invariant) directed transfer function. We have also examined the ability of the ADTF method to localize the sources of interictal spikes in a patient with epilepsy. As would be expected by using the MVAAR model with time-varying coefficients, the present results demonstrate that the ADTF method reveals dynamic information about the connectivity pattern that is missed when the conventional DTF and time-invariant MVAR model were used. Furthermore, due to this insufficiency in the consideration of the time-varying nature of information flow by the DTF, it sometimes provided erroneous results concerning the source of the propagated activity (Tables 1). This was also identified when the DTF method was applied to the patient interictal spike data (data not shown). The ADTF method, as indicated by our simulation results, is able to characterize various connectivity patterns, such as step functions (Fig. 4(a) and Fig. 9(a)), Gaussian functions (Fig. 5(a) and Fig. 8(a)), and oscillating function (Fig. 6(a)) and is tolerant to different SNR levels (Tables 1), which are within the typical range of ECoG measurement noise. Although it also indicates some biases (Fig. 8(a) and Table 1), they are extremely minor compared with the major dynamic connectivity patterns.

The ADTF method could potentially provide a useful tool in the analysis of the propagation of seizure and interictal activity since such propagation is obviously changing sharply over a short observation time window. In our present real ECoG data analysis, it shows promising results in localizing the primary sources of interictal spikes from an epilepsy patient (Fig. 10–Fig. 11). Note that the present ADTF results from interictal spikes did not identify the frontal focus, which was identified from ECoG recordings of seizure initiation (Fig. 10–Fig. 11). Thus, the present results should only be interpreted as a cross-examination of the ADTF method (in agreement with one ictal onset zone), and not judged upon clinical assessments based on ECoG seizure data. Further research will be needed in order to address the consistency of sources between interictal spikes and seizures, which is beyond the scope of the present study.

By analyzing the time-variant connectivity, it is also possible to identify the primary sources which initiate the seizure and to characterize the dynamics of propagations. More thorough understanding of seizure propagations could lead to improved clinical intervention, such as resecting certain propagation pathways instead of the entire epileptogenic zones close to the eloquent cortex which makes traditional resection risky or even impossible. Additionally, identification of the areas of cortex which drive seizure propagation and propagation pathways could potentially result in more favorable surgical outcome.

While we have focused on the DTF-based method, it is one of several connectivity estimators which is derived from the MVAR coefficients fit to a multivariate time series [19]. Such estimators could be easily adapted to take advantage of the time-varying model coefficients supplied by the MVAAR model. Development of techniques capable of estimating the rapid changes in connectivity networks could provide neuroscientists a useful tool in the study of dynamic cortical networks.

In summary, we have developed an adaptive directed transfer function method to study time-variant propagation of brain activity. The time-variant connectivity reconstruction is enabled by incorporating the Kalman filter algorithm into the multivariate auto-regression modeling. The simulation study and real ECoG data analysis indicate its efficacy in reconstructing various time-variant connectivity patterns associated with epileptiform activity. Additionally, this proposed method may also be applicable to other applications.

Acknowledgments

The authors would like to thank Dr. Wim van Drongelen for making the epilepsy data available, and Ms. Han Yuan for useful discussions. This work was supported in part by NIH RO1EB007920-01A1, RO1EB00178-05, NSF BES-0411898, and a grant from the Institute of Engineering in Medicine at the University of Minnesota.

References

1. Uhlhaas PJ, Singer W. Neural synchrony in brain disorders: relevance for cognitive dysfunctions and pathophysiology. *Neuron* 2006 Oct 5;vol. 52:155–168. [PubMed: 17015233]
2. Horwitz B. The elusive concept of brain connectivity. *Neuroimage* 2003 Jun;vol. 19:466–470. [PubMed: 12814595]
3. Lee L, Harrison LM, Mechelli A. A report of the functional connectivity workshop, Dusseldorf 2002. *Neuroimage* 2003 Jun;vol. 19:457–465. [PubMed: 12814594]
4. Babiloni F, Cincotti F, Babiloni C, Carducci F, Mattia D, Astolfi L, Basilisco A, Rossini PM, Ding L, Ni Y, Cheng J, Christine K, Sweeney J, He B. Estimation of the cortical functional connectivity with the multimodal integration of high-resolution EEG and fMRI data by directed transfer function. *Neuroimage* 2005 Jan 1;vol. 24:118–131. [PubMed: 15588603]
5. Andres FG, Gerloff C. Coherence of sequential movements and motor learning. *J. Clin. Neurophysiol* 1999 Nov;vol. 16:520–527. [PubMed: 10600020]
6. Leocani L, Comi G. EEG coherence in pathological conditions. *J. Clin. Neurophysiol* 1999 Nov;vol. 16:548–555. [PubMed: 10600022]
7. Kus R, Kaminski M, Blinowska KJ. Determination of EEG activity propagation: pair-wise versus multichannel estimate. *IEEE Trans. Biomed. Eng* 2004 Sep;vol. 51:1501–1510. [PubMed: 15376498]
8. Kaminski MJ, Blinowska KJ. A new method of the description of the information flow in the brain structures. *Biol. Cybern* 1991;vol. 65:203–210. [PubMed: 1912013]
9. Granger CWJ. Investigating causal relations by econometric models and cross-spectra methods. *Econometrica* 1969;vol. 37:424–428.
10. Franaszczuk PJ, Bergey GK, Kaminski MJ. Analysis of mesial temporal seizure onset and propagation using the directed transfer function method. *Electroencephalogr. Clin. Neurophysiol* 1994 Dec;vol. 91:413–427. [PubMed: 7529681]
11. Franaszczuk PJ, Bergey GK. Application of the directed transfer function method to mesial and lateral onset temporal lobe seizures. *Brain Topogr* 1998 Fall;vol. 11:13–21. [PubMed: 9758388]
12. Ding L, Worrell GA, Lagerlund TD, He B. Ictal source analysis: localization and imaging of causal interactions in humans. *Neuroimage* 2007 Jan 15;vol. 34:575–586. [PubMed: 17112748]
13. Arnold M, Miltner WH, Witte H, Bauer R, Braun C. Adaptive AR modeling of nonstationary time series by means of Kalman filtering. *IEEE Trans. Biomed. Eng* 1998 May;vol. 45:553–562. [PubMed: 9581053]
14. Campi M. Performance of RLS identification algorithms with forgetting factor: a phi-mixing approach. *J. Math. Syst. Estimation. Contr* 1994;vol. 4:1–25.
15. Schwarz G. Estimating the dimension of a model. *Ann. Stat* 1978;vol. 6:461–464.
16. Lutkepohl H. Comparison of criteria for estimating the order of a vector autoregressive process. *J. Time. Ser. Anal* 1985;vol. 6:5–52.
17. Palus M, Hoyer D. Detecting nonlinearity and phase synchronization with surrogate data. *IEEE Eng. Med. Biol. Mag* 1998;vol. 17:40–45. [PubMed: 9824760]
18. Theiler J, Eubank S, Longtin A, Galdrikian B, Farmer JD. Testing for nonlinearity in time series: the method of surrogate data. *Physica D* 1992;vol. 58:77–94.

19. Astolfi L, Cincotti F, Mattia D, Marciani MG, Baccala LA, de Vico Fallani F, Salinari S, Ursino M, Zavaglia M, Ding L, Edgar JC, Miller GA, He B, Babiloni F. Comparison of different cortical connectivity estimators for high-resolution EEG recordings. *Hum. Brain Mapp* 2007 Feb;vol. 28:143–157. [PubMed: 16761264]

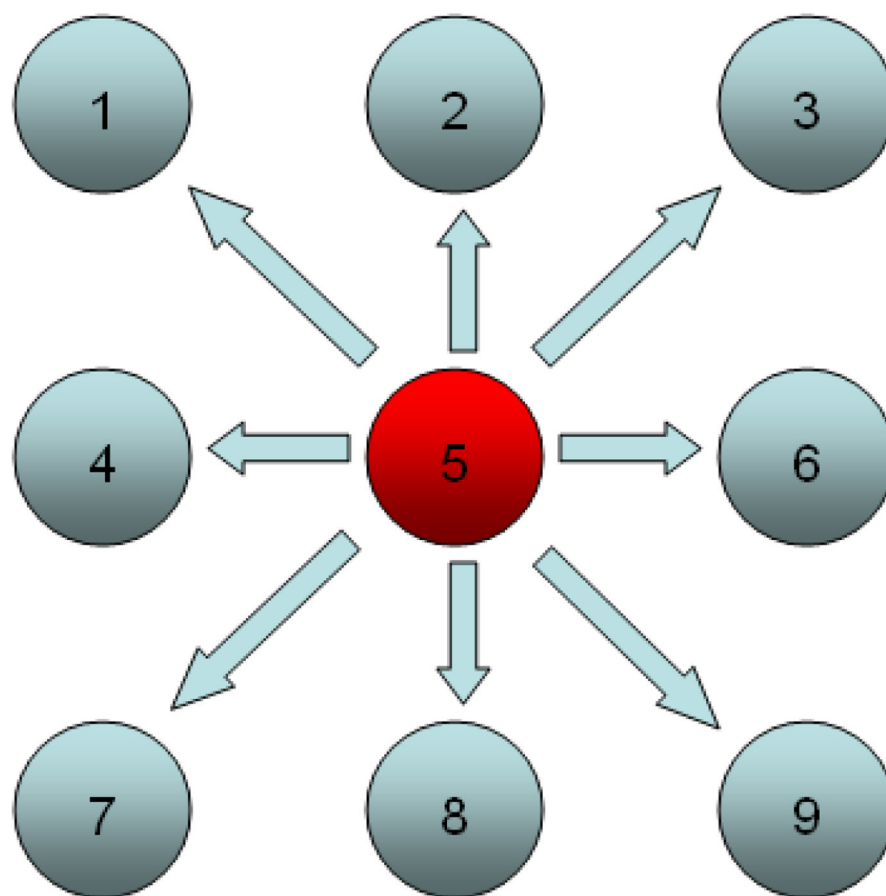
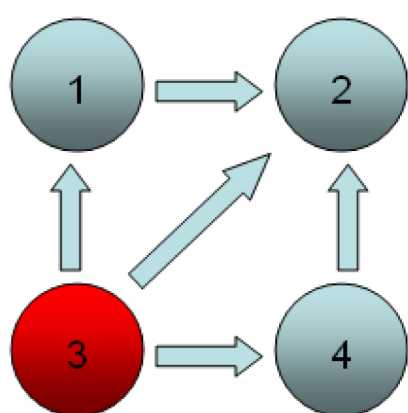
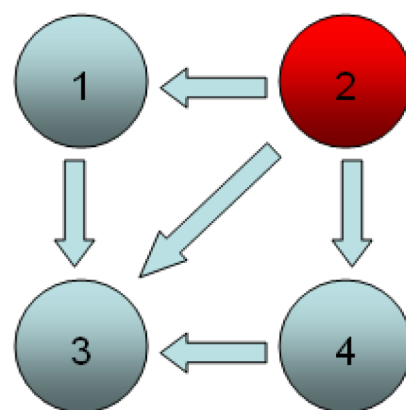


Figure 1. Graphical illustration of the second connectivity model. In this model, node 5 is the primary source of the activity (here an interictal spike) which propagates outward in a radial fashion.



(a)



(b)

Figure 2.

Graphical illustration of the third connectivity model. In this model, node 3 is the primary source of the sample seizure activity which then spreads to nodes 1, 2 and 4. Midway through the time series, the source of activity switches to the second node.

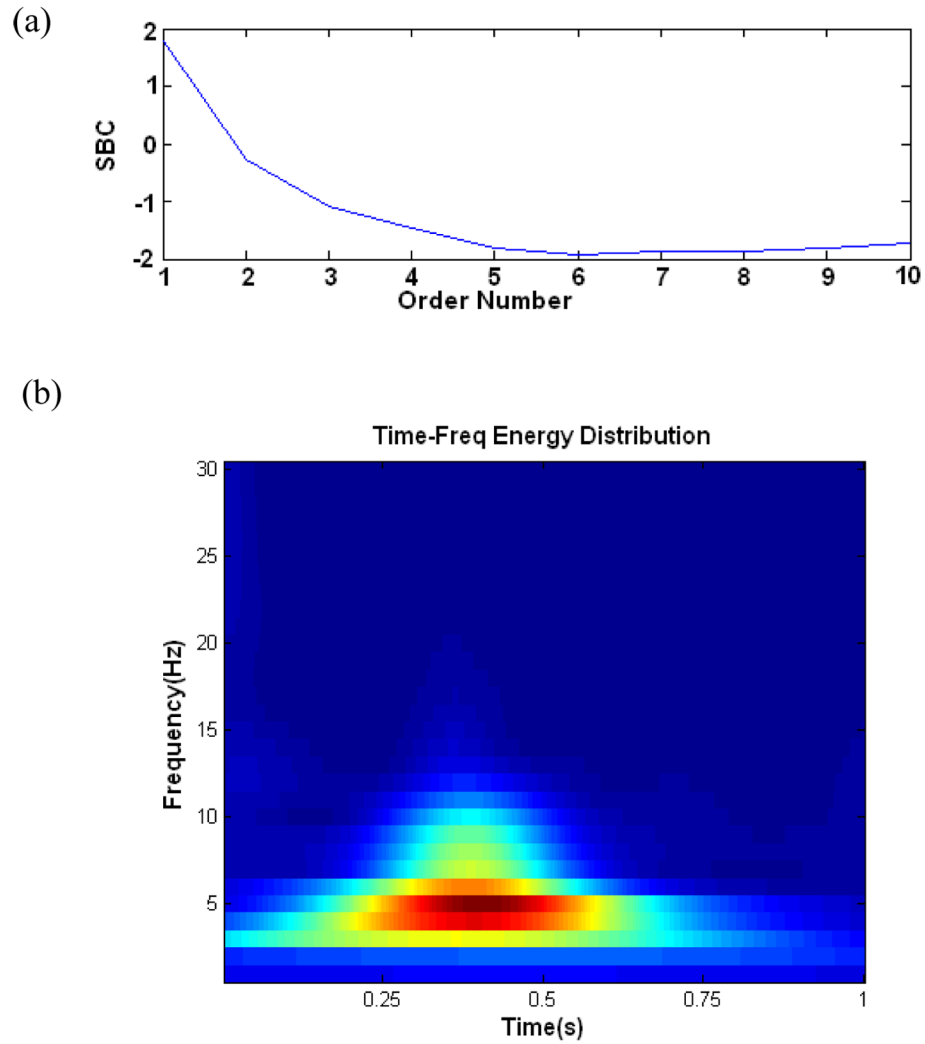


Figure 3.

(a) A plot of the SBC vs. model order for one of the interictal spikes from the patient data. Here it can be observed that the minimum SBC, and thus optimal model order is 6. (b) A time-series representation of an interictal spike from the patient data. The frequency band in which the ADTF/DTF values were integrated over was chosen by visual analysis of the spectral frequencies corresponding to the interictal spike.

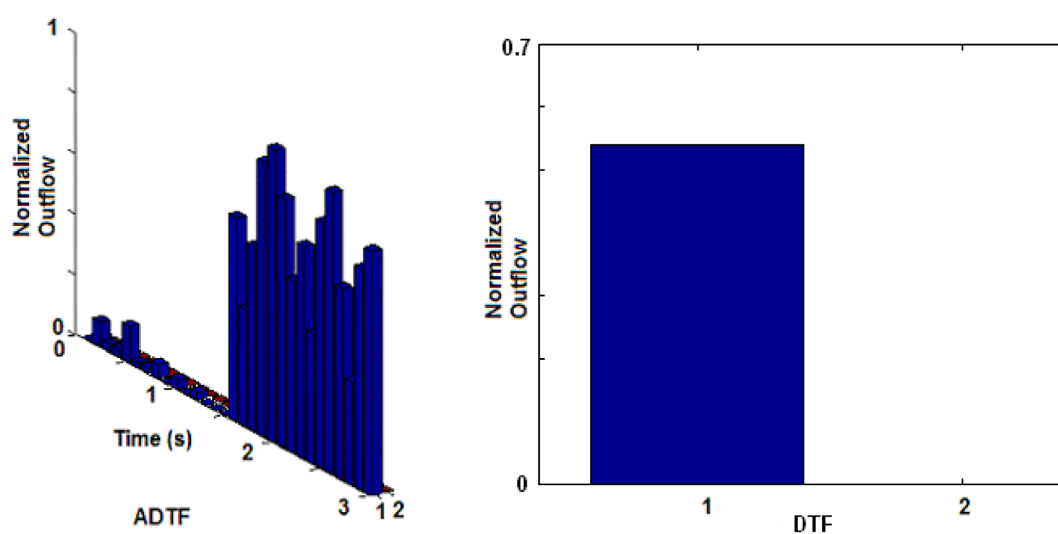


Figure 4.

The significant total outflow from the first propagation pattern of the first model at a SNR of 20 dB. (a) Time-variant (Heaviside function) connectivity reconstruction achieved by the ADF method. Each bar corresponds to the average ADF values over a 100 ms window; (b) Time-invariant connectivity reconstruction by the DTF method.

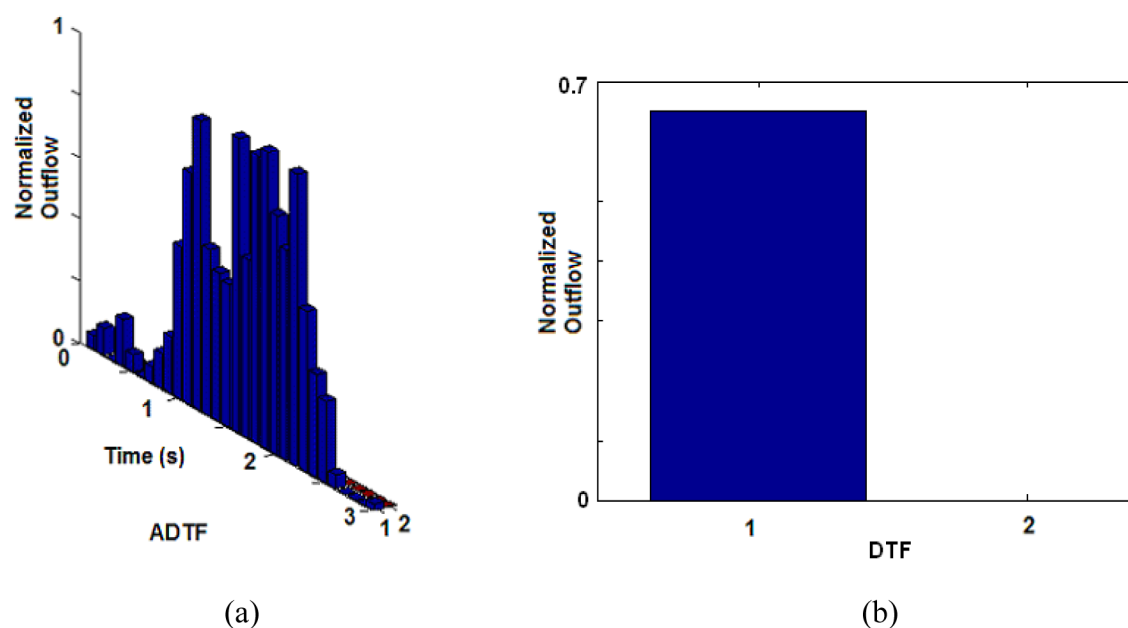


Figure 5. The significant total outflow from the second propagation pattern of the first model at a SNR of 20 dB. (a) Time-variant (Gaussian function centered at 1.5 s) connectivity reconstruction achieved by the ADF method; (b) Time-invariant connectivity reconstruction by the DTF method.

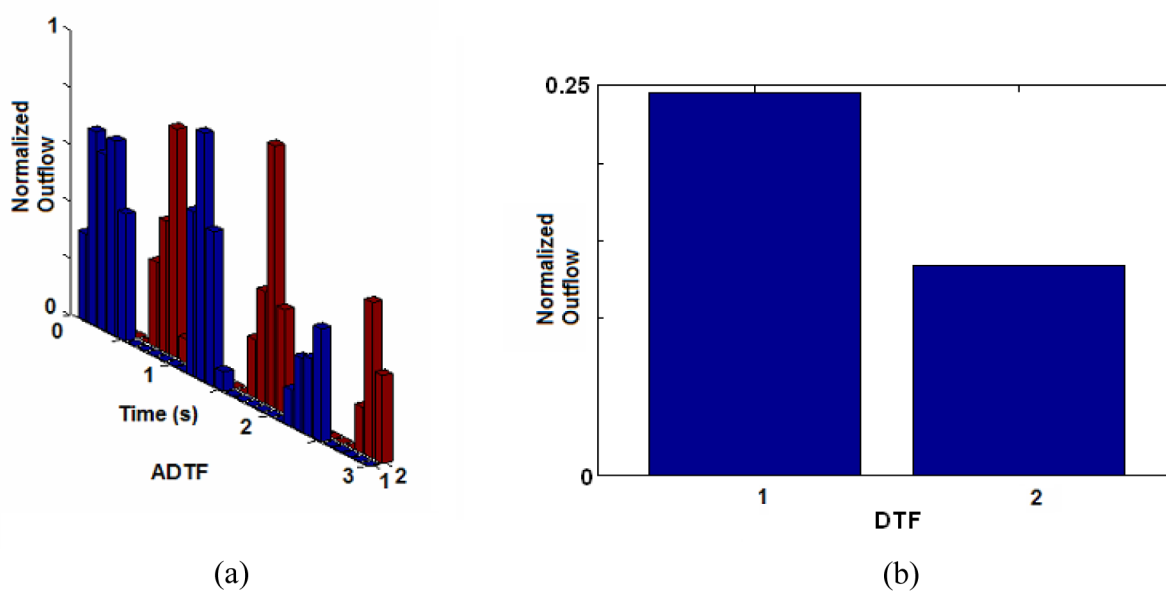


Figure 6.

The significant total outflow from the third propagation pattern of the first model at a SNR of 20 dB. (a) Time-variant (oscillating function with a 1 s period) connectivity reconstruction achieved by the ADF method; (b) Time-invariant connectivity reconstruction by the DTF method.

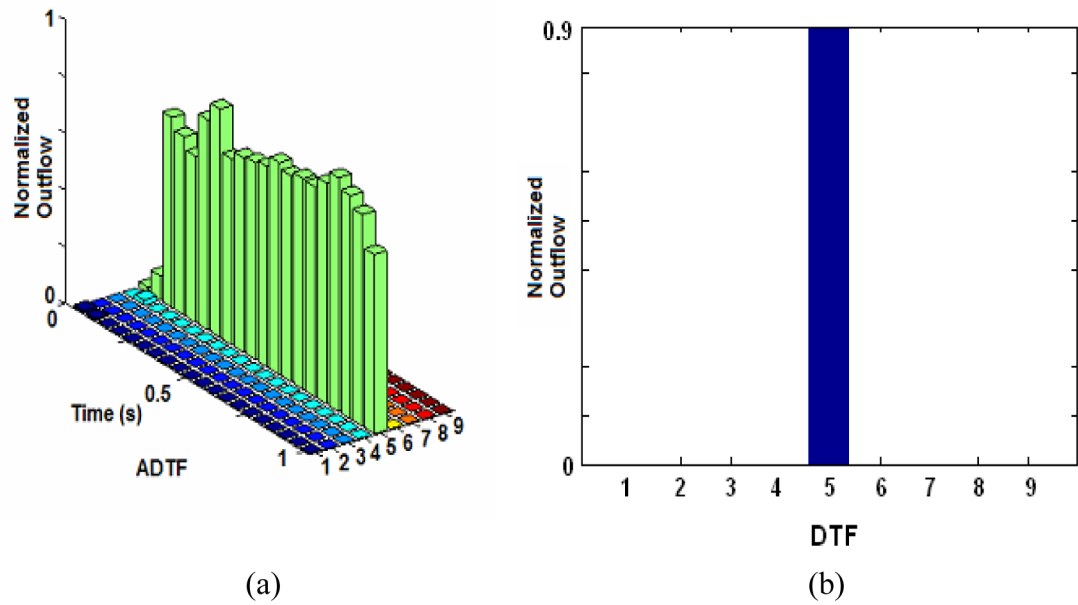


Figure 7.

The significant total outflow from the first propagation pattern of the second model at a SNR of 20 dB. Time-invariant connectivity reconstruction achieved by the ADF method (a) and the DTF method (b). Each bar of (a) corresponds to the average ADF value over a 50 ms window.

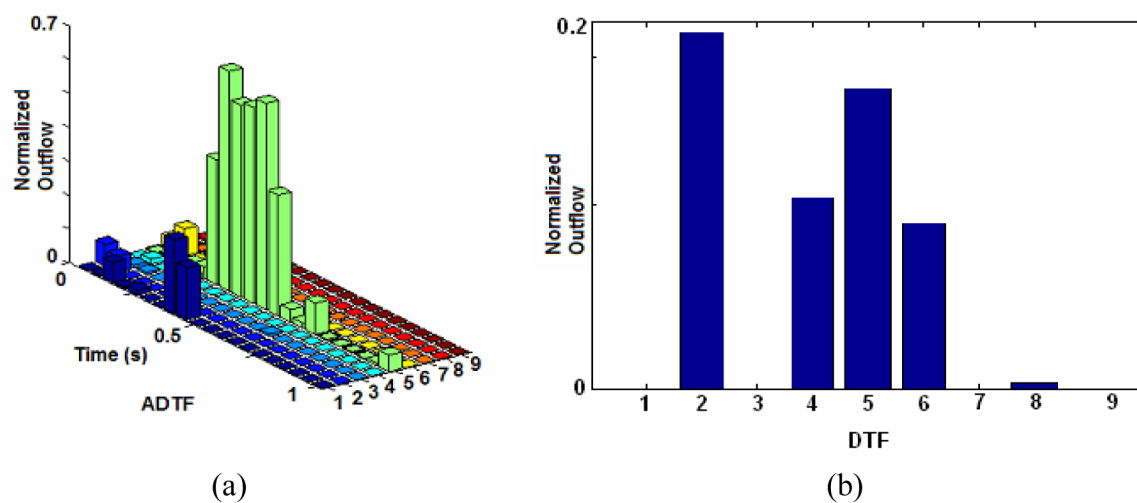


Figure 8. The significant total outflow from the second propagation pattern of the second model at a SNR of 20 dB. Time-variant connectivity reconstruction achieved by the ADF method (a) and the DTF method (b).

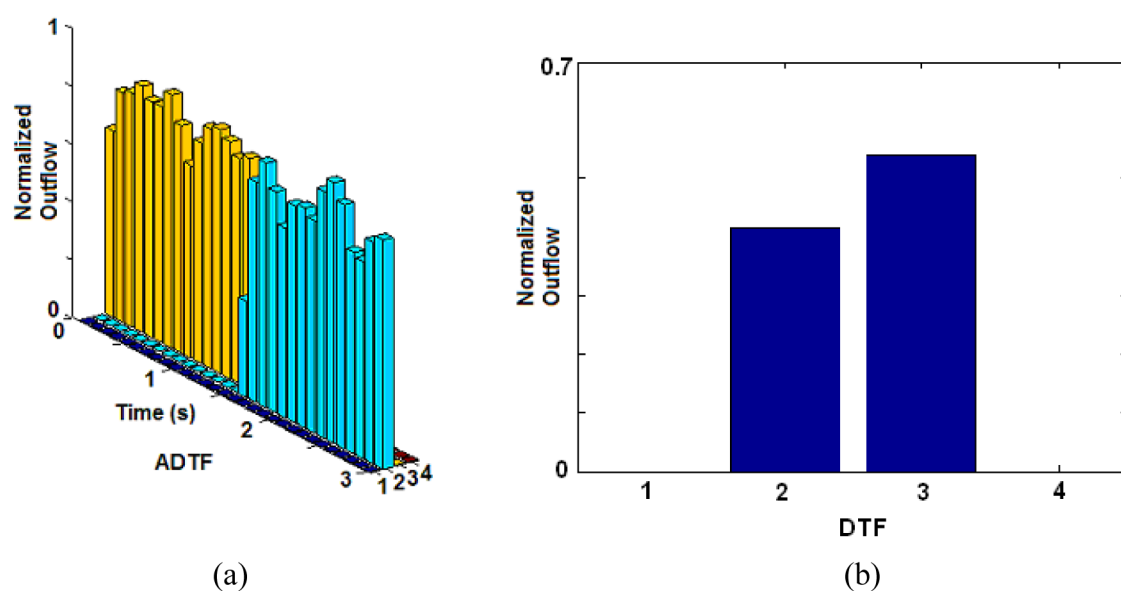


Figure 9.

The significant total outflow from the third model at a SNR of 20 dB. The ADTF (a) correctly distinguishes the third node as the initial primary source which then moves to the second node at the 1.5 s time mark. Each bar represents the average ADTF value over a 100 ms window. The DTF method (b), identifies both the second and third nodes as source of propagation.

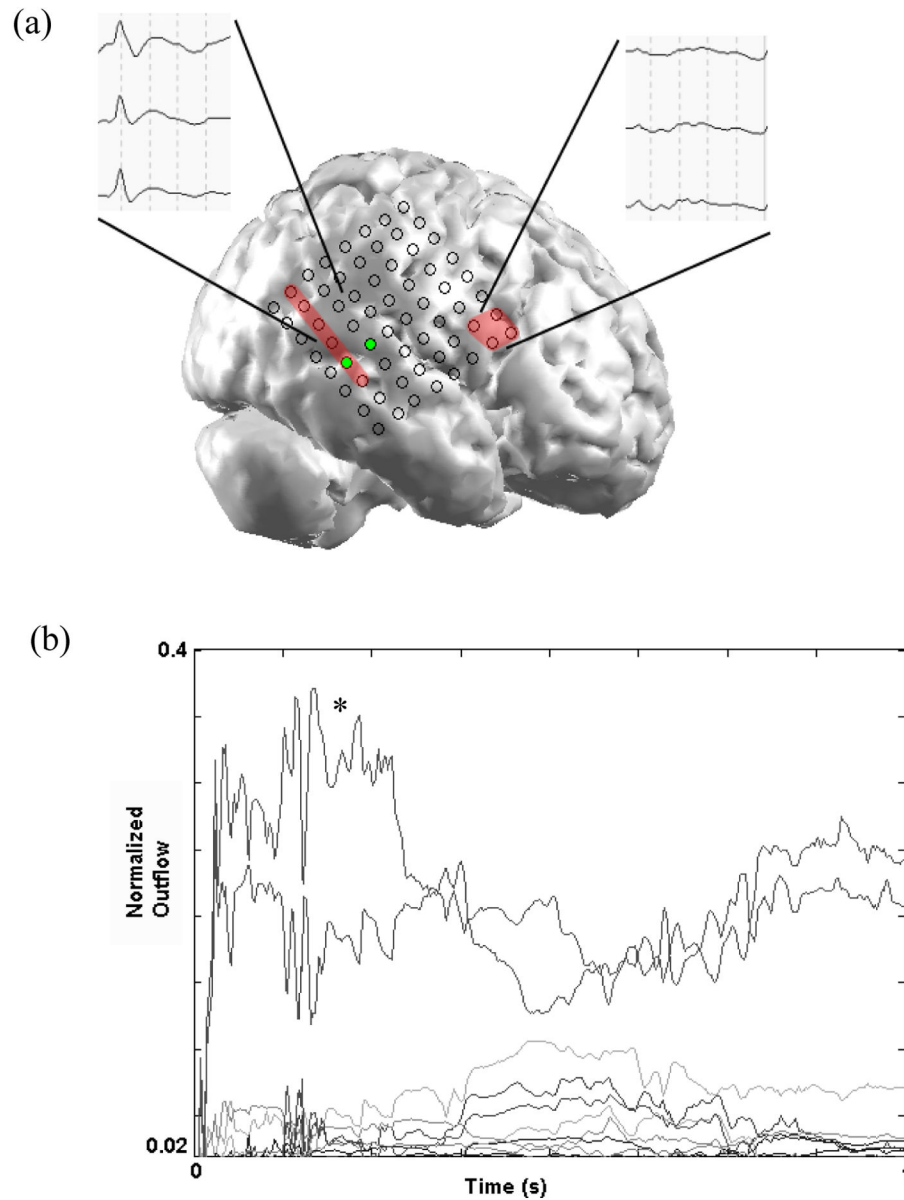


Figure 10.

(a) The maximum significant total outflow from a representative interictal spike recorded from a subdural ECoG grid in an epilepsy patient. (a) The ictal onset zones which were identified by the epileptologists based on ictal ECoGs are shown in red. Representative time series for each of the two focal areas are shown. While the interictal spike waveform was present over the posterior two-thirds of the ECoG grid, the frontal focus displayed little to no spiking activity. The nodes identified by the ADF method as sources are highlighted. (b) The time course of the ADF values for the interictal spike. The waveform indicated by the * corresponds to the identified source electrode within the seizure onset zone.

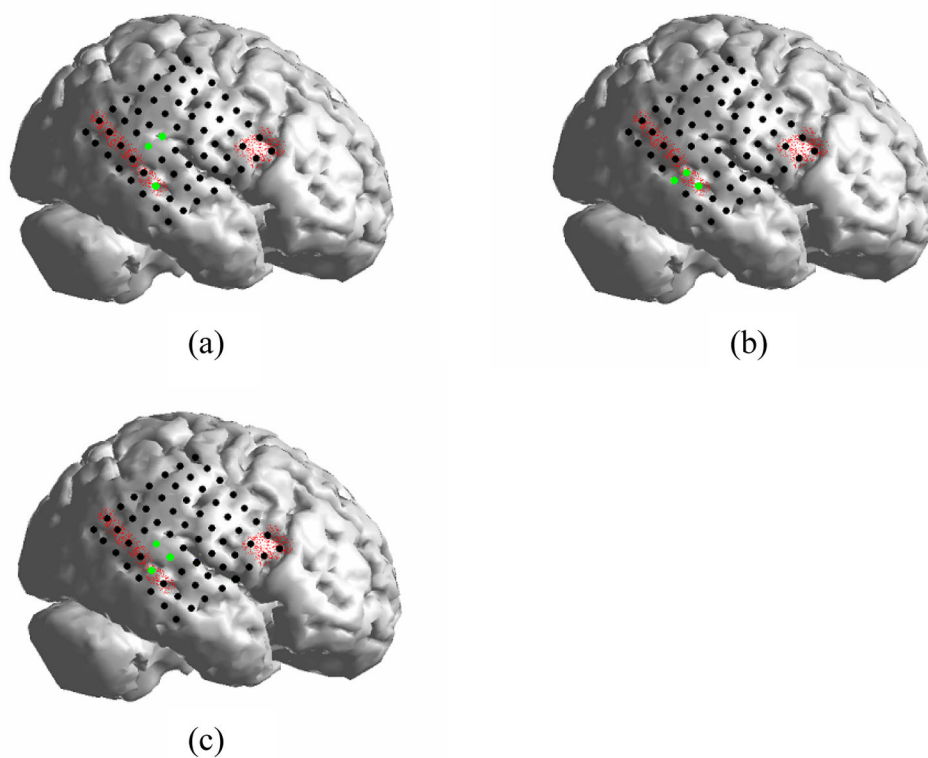


Figure 11.
The sources of outflow during three other interictal spikes (in the same patient) identified by the ADTF method.

Table 1

Computer simulation results obtained by the ADTF and DTF methods in the second model. Nodes were labeled as significant if they had >50% of the maximum outflow (both ADTF and DTF) and occurred during the interictal spike (ADTF only). When the connectivity pattern is static, both methods are equivalent in identifying only the fifth node as the source of activity. In the dynamic case, the ADTF correctly identified the fifth node as the source of activity. In the DTF method, multiple other nodes were identified as the primary source of the propagated activity.

Causality Function	SNR Level (dB)	Nodes with Significant Outflow	
		ADTF	DTF
Static causality	20	5	5
	15	5	5
	10	5	5
	5	5	5
Dynamic causality (Gaussian Function)	20	1,5	2,4,5
	15	5,7	1,5,6
	10	5	1,5,6,8
	5	5	1,5